Oceanic resurge deposits at the Rochechouart impact structure (France) suggest a marine target environment

Jens Ormö, Erik Sturkell, Philippe Lambert, Sylvie Bourquin, Jean-Baptiste Cherfils

Oceanic resurge deposits at the Rochechouart impact structure (France) suggest a marine target environment

Jens Ormö[1], Erik Sturkell[2], Philippe Lambert[3], Sylvie Bourquin[4] and Jean-Baptiste Cherfils[4]

[1]Centro de Astrobiologia (CAB), CSIC-INTA, Carretera de Ajalvir km 4, 28850 Torrejón de Ardoz, Madrid, Spain;
[2]Earth Sciences Centre, Gothenburg University, Gothenburg, Sweden; [3]Centre for International Research on Impacts and on Rochechouart (CIRIR), 2 Faubourg du Puy du Moulin, Rochechouart 87600, France and
[4]University of Rennes, CNRS, Géosciences Rennes – UMR 6118, F-35000, Rennes, France

Abstract

The Rochechouart impact structure, located in the western part of the Massif Central in France, has been suggested to be one of the largest impact structures in western Europe. Various age datings have placed the event in a span from the Late Triassic to the Early Jurassic, but the most recent works favour a Late Triassic age. Very little is known about the target environment at the time and location of the impact event. Seemingly coeval, potential tsunamites along palaeoshorelines of the sea that covered parts of continental Europe at the time have been suggested to be related to the impact event and may indicate a marine target setting. Here we apply the method of visual line-logging of the graded suevite in the Chassenon SC2 drill core. This method has previously been used to investigate the depositional environment of similar deposits in several marine target impact craters. It allowed us to compare the deposits at these craters with those at Rochechouart, and in this way not only confirm the marine target setting, but also estimate the target water depth to be ~200 m. Altogether, our results indicate a palaeogeographic target setting in a newly opened seaway connecting the Paris Basin with the Aquitaine Basin, which may indicate an age of impact at the younger end of the hitherto suggested age-span, i.e. in the late Rhaetian – Early Jurassic.

1. Introduction

The Rochechouart impact structure is located near the NW edge of the French Massif Central (Limousin region; Fig. 1), and has been suggested to measure at least 12 km across based on the extent of the allochthonous breccia deposits (Lambert 1977), with an original crater diameter estimated to have been more than 15 km (Kraut & French, 1971). A gravity survey by Pohl et al. (1978) indicated an original diameter of 10–20 km, whereas other studies have proposed even larger crater diameters, such as 32 km (Osinski & Ferrière, 2016), and up to 40–50 km (Lambert, 2010). Nevertheless, a deep erosional level is expected, considering that c. 1100 m of basement rocks have been eroded since exhumation was initiated in the Early Cretaceous (François et al. 2020). The crater infill sequence is, at least locally, remarkably complete at Chassenon (north-central part of the area of impactites) where a fine-grained, impactoclastic layer is locally found overlying a graded suevite, landmarking the top of the sequence (Lambert, 2010) (Fig. 1). To obtain a better view of the sequence at Chassenon, three holes were cored as part of the 2017 drilling programme (Lambert et al. 2018). The longest of these cores, the 121.7 m deep SC2 hole, is described by Lambert et al. (2018) to intersect 88 m of suevite and 25 m of basement breccia that seems to have a downward transition into more intact gneissic basement rocks (Fig. 2). This core does, however, not include the impactoclastite layer, which therefore is not within the scope of this study.

The age of the impact event has been subject to discussion (see Rasmussen et al. 2020). An age estimate based on isotopic techniques was obtained from outcropping impact melt rock at the Babaudus locality by Reimold and Oskierski (1987), which was 185.5 ± 2.2 Ma. Preliminary K–Ar ages of 150–170 Ma had already been presented from the same locality by Kraut and French (1971). Later, from a pseudotachylyte sample from the Champagnac Quarry, Kelley and

Spray (1997) proposed a $^{40}Ar/^{39}Ar$ age of 214 ± 8 Ma. However, Schmieder et al., 2010, 2014) suggested this age was presumably too old and they obtained an $^{40}Ar/^{39}Ar$ age of 201 ± 2 Ma from recrystallized K-feldspar in strongly impact-metamorphosed gneiss found near Videix, i.e. western-central domain of the Rochechouart structure. This age was then determined as 202.7 ± 2.2 Ma (recalculated in Jourdan et al. 2012) or 203 ± 2 Ma (Cohen et al. 2017, using the decay constants and Fish Canyon sanidine standard age from Renne et al. 2011). Cohen et al. (2017) running $^{40}Ar/^{39}Ar$ analysis of a surface sample of impact melt rock collected in Babaudus, obtained an age of 206.92 ± 0.20/0.32 Ma, and concluded that the Rochechouart impact structure predates the Triassic–Jurassic boundary by 5.6 ± 0.4 Ma and so is not temporally linked to the Triassic– Jurassic mass extinction. However, the relatively high age obtained by those authors could possibly be influenced by the incorporation of ^{40}Ar from the target rocks (cf. Jourdan et al. 2007). In addition, Horne (2016) found a U–Th/He age of 191.6 ± 9.1 Ma (from the Montoume breccia and Babaudus impact melt rock) and two laser ablation – inductively coupled plasma – mass spectrometry (LA-ICP-MS) U–Pb age populations of 202.6 ± 5.8 Ma and 211 ± 13 Ma (from the Montoume breccia). More recently, Rasmussen et al. (2020), by applying U–Pb depth profiling on the same Babaudus impact melt of Cohen et al. (2017), demonstrated that what is known as Former Reidite in Granular Neoblastic (FRIGN) zircon supports preserving a time of impact of 204–207 Ma. However, these authors found a younger age of 194 ± 2.9 Ma supporting the younger ages suggested by Horne (2016) and Reimold and Oskierski (1987), which they link to a post-impact thermal event unrelated to the impact. In consequence, even if a Late Triassic age is considered to be the current best estimate of the Rochechouart impact, an age a few million years younger cannot be excluded.

The location of the impact relative to the palaeo-sea is currently unknown as no marine sediments are known to cover the Variscan crystalline basement in the area. However, thin conglomerates have been suggested to have covered the Triassic peneplaine prior to the onset of marine sedimentation during the Early Jurassic (e.g. Cathelineau et al. 2012). Schmieder et al., 2010) suggest that the impact occurred in a near-coastal to shallow marine location between the Tethys Ocean in the south and the Rhaetian Sea to the north, following a transgression initiated during the late Norian (e.g. Bourquin et al. 2002) or Rhaetian (e.g. Goldsmith et al. 2003). Schmieder et al., 2010) further support this hypothesis by providing a review of published observations of potential seismites and tsunamites along palaeoshorelines of the Rhaetian Sea as far apart as southern France (e.g. Mader, 1992) and the British Isles (e.g. Simms, 2007), as well as of marine geochemical components in pseudotachylites at the Rochechouart crater (Kelley & Spray, 1997).

Relatively thick graded deposits of often suevitic character (i.e. significant melt particle content) are known to represent the uppermost parts of the impact-generated infill sequences in marine target craters, e.g. Lockne, Tvären, Chesapeake Bay, Flynn Creek, Wetumpka, Chicxulub (see summary in Ormö et al. 2021). Visually, the graded suevite in SC2 shows many similarities with such deposits that formed by the oceanic resurge during the early stage of crater modification (cf. Ormö et al. 2007). Here, we present results from visual core logging of the graded suevite in SC2. With this we aim not only to show the mode of deposition of the graded suevite in the Rochechouart crater, but also provide an assessment of the palaeogeography and timing of the impact event.

2. Methods

We have applied the same line-logging technique on the SC2 core as has been used on cores from several other marine target craters (e.g. Ormö et al. 2007, 2009, 2021). A line is drawn along the core, and the granulometry and lithology of every clast ≥5 mm that touches the line are determined visually with standard geological field techniques (e.g. Coe et al. 2010). In this study we note clast lithology, frequency, size, sorting, and roundness, both general and lithology-specific, and then treat this statistically as variations per metre length of the core. A total of 6002 clasts were logged and first separated into 18 distinctive sub-classes. For simplicity, these were then grouped into four main classes: (1) melt particles (brown, green and white); (2) gneiss (includes various lithologies determined to be part of the gneiss suite of the area); (3) granite; and (4) a small group of exceptionally well-rounded lithic clasts (hereafter EWRLC) (Fig. 3). The applied method allows evaluation of the target environment (i.e, aquatic or land) by analysing the sedimentology of the clastic deposits in the SC2 core in

comparison with known marine target craters studied using the same method. A more detailed study of the clast lithologies (e.g. the potential variations among the melt particles) is beyond the scope of this study. The emphasis is instead on their relative variations along the core.

3. Results

The results from the line-logging and statistical analysis are presented in Fig. 4. Of the 6002 logged clasts 63.6 % are gneiss, 10.9 % granite, 18.4 % green melt, 5.5 % white melt, 0.9 % brown melt and 0.6 % EWRLC. The lithologies of the 38 EWRLC clasts are either igneous (granitic with mainly milky quartz) or metamorphic (quartzite) (Fig. 3), likely originating from a thin, reworked residue after the Permian–Triassic weathering of the crystalline basement described by Cathelineau et al. (2012). Further rounding of the clasts may have occurred by fluvial or shoreline processes. It is important to note that no clasts of sedimentary rock have been detected. Clasts that represent direct lithological fragments of the target (i.e. gneiss, granite and EWRLC) occur relatively evenly throughout the logged section (Fig. 4). The most obvious variation is seen for the melt particles. Below 88 m melt particles are nearly absent. At 88 m there is a sudden increase, and up to 38.9 m the amount varies around 17 % with a peak at c. 80 m and a low at 60 m. At 38.9 m there is another sudden increase to c. 45 % that, with some fluctuations (25 m, 15 m, 5 m), continues to the top of the core. There is also a clear variation in the colour of the melt particles (e.g. white is more common at levels with relatively high melt clast abundance), but the reason for the colours of the melt particles is not analysed any further in this study.

The size sorting throughout the logged section fluctuates around a mean of c. 1, i.e. moderately to poorly sorted (Folk, 1974). Clast frequency, size and sorting are related to each other as follows:

In the zone between 105 m and 103 m the curves obtain some structure after having been completely chaotic below 105 m. Clear reverse grading (i.e. upwards increase in clast size, but reduction in clast frequency and sorting) occurs between 103 m and 79 m. There then follows a normally graded interval 79−61 m. In the interval 61−39.8 m there is again a decrease in the number of clasts towards the top. As this is not accompanied by an increase in clast size it is more likely a consequence of increased matrix content (i.e. mud). At 61 m, or possibly even as early as 63 m, the first significant change in roundness occurs, with a general increase in angularity towards the top of the 61−39.8 m interval. A drastic shift in the clast frequency (increase), size (increase), sorting (reduction) and lithology (high melt particle content) occurs at 39.8 m. However, this is followed by a normal graded sequence. The size sorting also gradually increases upwards. This interval also sees a general increase in the amount of melt, notably white and brown melt.

In the interval 39.8−0 m there then occurs a set of repetitions in clast frequency and size, although sorting generally improves until a fluctuation occurs at 6 m below the top of the logged section. At 33 m, roundness shows a distinct increase, but then again decreases slightly to the top until the topmost 6 m where it again shows a distinct fluctuation.

The uppermost 6 m of the core is characterized by a drop in clast frequency coupled with an increase in clast size, as well as poorer sorting. As the clasts are still mainly larger than the 5 mm cut-off, this grain-size drop is considered to be real and not an artefact (cf. Ormö et al. 2007, 2021). Altogether, this indicates increased matrix content. The higher angularity of clasts is coupled with the increased melt content, which includes more brown melt. This is distinctively different from that of the impactoclastite layer described by Lambert (2010) as 'ash-like horizontal deposit of very glass-poor, fine-grained, lithic debris derived from basement rocks'. Instead, it is more likely a strongly mud-charged suspension flow with angular, more distal (i.e. higher shocked) ejecta. It is common for the finer-grained top parts of resurge deposits to have a higher content of shocked material (Therriault & Lindström, 1995). At Chicxulub, increased angularity is coupled with an increased amount of melt fragments, possibly forming shards after rapid quenching in contact with seawater (Osinski et al. 2020). The circle diagrams in Fig. 5 show that also at Rochechoart the melt clasts express a high angularity. Likewise, the granite clasts show a higher angularity than that of the gneiss (possibly an effect of rheology), but they are relatively few and evenly distributed along the core, thus not affecting the general roundness graph to the same degree.

4. Discussion

4.a. Palaeoenvironmental implications

There are clear trends in the data graphs (Fig. 4), which allow comparisons with published data on cores from other craters with similar deposits (see review in Ormö et al. 2021). Of those, the Lockne-2 core is most similar with respect to clast frequency, size and sorting variations (Fig. 4). In addition, the Chicxulub M0077A core also shows conspicuous similarities with respect to lithology distribution and roundness variation (cf. Ormö et al. 2021). The chaotic appearance of the curves below 105 m indicates avalanche and slump deposits with little or no influence from water. However, the organization that occurs in the interval 105−103 m is known from previously studied craters to indicate an often relatively short transition zone in which there is an initiation of transport and deposition in water (e.g. Ormö et al. 2007, 2009, 2021; Sturkell et al. 2013). Figures 4 (right column) and 6 describe the depositional process and the dynamics of the water flow; deposition out of suspension begins at 103 m and then dominates upwards. The upwards following trends are also seen in the relatively deep-marine resurge deposits at Lockne (target water depth H ~ 500 m), but also to some extent at Chicxulub (H ~ 2000 m). At both Lockne and Chicxulub, a forceful resurge passed in over the crater floor, causing mainly rip-up and traction along the floor, but little deposition (i.e. the transition zone 105−103 m). At Lockne, where water can enter from all directions, a 'Central Water Plume' (CWP) forms. It is after the collapse of the CWP and the initiation of an anti-resurge that the major deposition begins (Ormö et al. 2007). A mud-rich deposit carrying a high amount of basement rip-up clasts is dumped rapidly when the transport energy temporarily drops. This is followed by oscillations within the crater causing a set of repeated beds although with a general fining-up. At Chicxulub there is no indication of the formation of a CWP. However, a collision of flows diverted around the peak ring caused a second pulse in energy with similar consequences to the deposition. All in all, the granulometry displayed in the Rochechouart SC2 core from 103 m depth and to the top is typical for a suspension deposit created bya forceful flow capable of keeping a huge amount of material in suspension (cf. Ormö et al. 2021).

At Lockne, the combination of target and relative water depth did not generate any melt particles of sizes above the 5 mm cut-off. However, in Unit 2 in the Chicxulub M0077A core the amount, size distribution and shapes of melt particles are similar to those of the SC2 core. For Chicxulub, Ormö et al. (2021) suggested the melt particles to, at least partially, originate from interaction between the resurge and large melt pools on the crater floor ('Melt-Water-Interaction, MWI', cf. Osinski et al. 2020). Notably, at Chicxulub angular clasts (also here often melt particles) are kept longer in suspension than rounded clasts (Ormö et al. 2021).

Deposits such as in SC2, Lockne-2 and Chicxulub M0077A indicate a transport as hyperconcentrated flows (see discussion in Ormö et al. 2021). This means a flow with 20–60 vol. % of material in suspension (Vallance, 2000). Considering the relatively low amount of clasts per metre (an average of 58) in SC2 compared with Lockne-2 (85) and Chicxulub M0077A (72) (cf. Ormö et al. 2021) despite a similar mean clast size, most likely the sediment load was at the higher end of that span. Assuming a sediment load of 50 vol. % for the Rochechouart resurge, the overall thickness of the SC2 resurge deposits (>103 m) would indicate a flow depth of ~200 m. Numerical simulations of resurge flows at Lockne and Tvären indicate that the depth of the target sea would be in the same order (Ormö et al. 2010). Less water, if at all able to pass the elevated rim, would have generated a complex set of debris flows similar to relatively shallow-water impacts such as Wetumpka (King et al. 2006; Ormö et al. 2021).

After having established that the deposits in the SC2 core require a significant amount of water for the transport we can conclude that the Rochechouart impact occurred in a marine setting. A water depth of 200 m is plausible for such a seaway over the Massif Central (J Fischer, pers. comm. 2021). However, the absence of any sediment clasts in the SC2 resurge deposits indicates that there may not have been enough time between the transgression and the impact for the formation of substantial volumes of lithified sedimentary rock.

4.b. The case for a nearshore impact event, and possible size of the crater

In a conceptual reconstruction of the process of water resurge we have placed a complex crater in a nearshore position (Fig. 6). The distribution of potentially water-deposited suevite within the Rochechouart crater indicates that deeper water was located to the west or the northwest (Fig. 2). When the resurge from the oceanic side passes in over the crater floor it may, in analogy to what is suggested for Chicxulub (e.g. Ormö et al. 2021), cause rip-up and MWI processes when interacting with the impact breccias and large melt pools that still today are visible in the crater interior (Fig. 1). When the resurge reaches a major topographic obstacle such as a central peak, or the far end of the crater, the reflected wave would generate a similar anti-resurge effect to that seen in Chicxulub and in the collapse of the CWP at Lockne (cf. Ormö et al. 2021). As no melt bodies are seen at the SC2 site, any MWI at Rochechouart likely occurs somewhere away from the SC2 location, possibly from the larger melt pools today seen further to the east (Fig. 1). Melt particles would then be transported to the SC2 site in suspension, and, as at Chicxulub, angular fragments are kept longer in suspension. While the crater continues to fill up, a second pulse of higher flow energy reaches the SC2 site, causing the increase in transport energy seen at 39.8 m (Figs. 4, 6). The water infill continues in a set of oscillations and seiches similar to what is described from Lockne and Chicxulub. Later erosion leaves the structure and impactite distribution seen today (François et al. 2020).

In addition, providing important evidence for a marine target environment, sedimentological studies of resurge deposits from marine target craters by Ormö et al. (2021), and further mathematical analysis by Herreros and Ormö (2022), indicate a relation between mean clast frequency (<N>), impactor diameter (d) and target water depth (H) that allows the estimate of any of these variables when the two others are known through independent sources. Equation 1 represents a location of the cored sediment in a low position of the crater (e.g. moat), and Equation 2 represents a relatively high position in the crater (e.g. central uplift area), or possibly a more turbulent position (Ormö et al. 2021; Herreros & Ormö, 2022):

$$< N > \frac{1}{4} -15\delta d=H\text{Þ} \text{Þ} 100 \quad (1)$$

$$< N > \frac{1}{4} -13\delta d=H\text{Þ} \text{Þ} 150 \quad (2)$$

Applying Equation 1 with <N> = 58, H = 200 m gives a projectile size of ~560 m, and for Equation 2 it is 1400 m. Tagle et al. (2009) argue that the impactor at Rochechouart most likely was an iron asteroid. A 600 m iron projectile gives, according to the impact-effect calculator down2earth.eu (accessed May 2021) a crater diameter of 13 km for an impact velocity of 18 km s^{-1} at 45° impact angle into a target of igneous rock. This would correlate with the distribution of impactites in the Rochechouart structure (Fig. 1). The same calculation for a 1400 m iron projectile gives a crater diameter of 28 km, which is similar to other suggested crater diameters (see Introduction). However, considering the relatively short core drillings, the scarcity of detailed geophysical data, the current lack of independent data on the target water depth, and the uncertainty of the position of the SC2 drill site relative to the pre-erosion geomorphology of the fresh crater, at this stage there are too many uncertainties for the results to be conclusive concerning the size of the fresh crater. The crater diameters obtained here can thus only be seen as indicative.

4.c. Palaeogeographical implications

Depending on the age considered, i.e. Rhaetian or Early Liassic (see Introduction), the palaeogeographic reconstructions will differ. For the Late Triassic, Scotese and Schettino (2017) consider that the marine Rhaetian sandstones, i.e. deltaic, are limited east of the Paris Basin. However, Bourquin et al. (1997, 2002) and Fischer et al. (2012) show that the restricted marine Rhaetian Sandstones grade westward to dolomitic coastal sabkha. i.e. brackish deposits, and to fluvial lacustrine deposits. During the Rhaetian, Bourquin et al. (1997, 2002) describe the first connection between the Paris and England basins and a new depocentre southwest of the Paris Basin, i.e. south of Tours, with maybe a connection of the fluvial sedimentation area

with the Aquitaine Basin (Fig. 7). In that area, Rauscher et al. (1992) and Merzeraud et al. (1999, 2000) consider Rhaetian fluvial deposits to be influenced by marine waters and connected with a coastal plain, and that the marine influence increased during the Early Liassic with mainly coastal plain environments grading laterally to calcareous marine deposits. In consequence, a possible connection between the Paris and Aquitaine basins could be envisaged in particular during the Early Jurassic (Fig. 8) following the major marine Sinemurian flooding in this area (cf. Cathelineau et al. 2012). The Sinemurian spans c. 6.6 Myr (Cohen et al. (2013). In the Aquitaine Basin, during the end of the Triassic and the early Early Jurassic, i.e. Rhaetian to Hettangian, brackish sedimentation is observed in the Aquitaine Basin (i.e. Dercourt et al. 2000; Boiron et al. 2002). In the area of Rochechouart (Fig. 7), only Rhaetian fluvial deposits outcrop in the Brive area (Astruc et al. 1995) and the Hettangian sedimentation is characterized by palustrine or lagoon deposits (Le Pochat et al. 1986; Astruc et al. 1995). In conclusion, given that the impact according to our estimates occurred under ~200 m of marine water, either the palaeogeographic reconstruction of the Rhaetian must be reconsidered, or the impact would have occurred in the Early Jurassic after a rapid enough transgression not to produce any consolidated sediments or calcareous mud of any quantities detectable by applying HCl to the core.

5. Conclusions

Sedimentological analysis of the suevite deposits at the SC2 core near Chassenon gives evidence for a shallow marine target environment for the Rochechouart impact with ~200 m water depth. More generally the Rochechouart impact can be used to further constrain the palaeotopography, palaeoenvironment and erosional history of the western edge of the French Massif Central. Likewise, our results would, in the current view of the Rhaetian palaeogeography, indicate an age of formation during the Early Jurassic. In any case, the obvious marine target setting calls for further attention to the date of the event.

Acknowledgements. The work by JO was supported by grants ESP2017-87676-C5-1-R and PID2021-125883NB-C22 by the Spanish Ministry of Science and Innovation/State Agency of Research MCIN/AEI/10.13039/501100011033 and by 'ERDF A way of making Europe', the Spanish State Research Agency (AEI) Project No. MDM-2017-0737 Unidad de Excelencia 'María de Maeztu'–Centro de Astrobiología (CAB) CSIC-INTA, the Spanish Research Council (CSIC) support for international cooperation: I-LINK project LINKA20203, and Centre for International Research on Impacts and Rochechouart (CIRIR). PL was supported by the CIRIR funds from the local communities of 'Porte Océane du Limousin' and 'Charente Limousine'

References

Astruc JG, Cubaynes R, Fabre JP, Galharaghe J, Lefavrais-Raymond A, Marcouly R, Pélissié T, Rey J and Simon-Coinçon R (1995) Notice explicative, Carte géol. France (1/50 000), feuille Soullac (809). Orléans: BRGM, 76 pp.

Boiron MC, Cathelineau M, Banks DA, Buschaert S, Fourcade S, Coulibaly Y, Boyse A and Michelot JL (2002) Fluid transfer at a basement/cover interface. Part II: large-scale introduction of chlorine into the basement by Mesozoic Basinal brines. Chemical Geology 192, 121–40.

Bourquin S, Robin C, Guillocheau F and Gaulier J-M (2002) Three-dimensional accommodation analysis of the Keuper of the Paris Basin: discrimina- tion between tectonics, Eustasy, and sediment supply in the stratigraphic record. Marine and Petroleum Geology 19, 469–98.

Bourquin S, Vairon J and Le Strat P (1997) Three-dimensional evolution of the Keuper of the Paris Basin based on detailed isopach maps of the strati- graphic cycles: tectonic influences. Geologische Rundchau 86, 670–85.

Cathelineau M, Boiron M-C, Fourcade S, Ruffet G, Clauer N, Belcourt O, Coulibaly Y, Banks DA and Guillocheau F (2012) A major Late Jurassic fluid event at the basin/basement unconformity in western France: $^{40}Ar/^{39}Ar$ and K–Ar dating, fluid chemistry, and related geodynamic context. Chemical Geology 322, 99–120. doi: 10.1016/j.chemgeo.2012.06.008.

Coe A, Argles T, Rothery D and Spicer R (2010) Geological Field Techniques. Chichester: Wiley Blackwell in association with the Open University. 336 pp. ISBN 978-1-4443-3062-5.

Cohen BE, Mark DF, Lee MR and Simpson SL (2017) A new high-precision $^{40}Ar/^{39}Ar$ age for the Rochechouart impact structure: at least 5 Ma older than the Triassic–Jurassic boundary. Meteoritics and Planetary Science 52, 1600–11. doi: 10.1111/maps.12880.

Cohen KM, Finney SC, Gibbard PL and Fan J-X (2013 [updated]) The ICS international chronostratigraphic chart. Episodes 36, 199–204.

De Marchi L, Ormö J, King DT Jr, Adrian DR, Hagerty JJ and Gaither TA (2019) Sedimentological analysis of two drill cores through the crater moat- filling breccia, Flynn Creek impact structure, Tennessee. Meteoritics and Planetary Science 54, 2864–78. doi: 10.1111/maps.13393.

Dercourt J, Gaetani M, Vrielynck B, Barrier E, Biju-Duval B, Brunet MF, Cadet JP, Crasquin S and Sandulescu M (2000) Atlas Peri-Tethys – Paleogeographical Maps. Paris: CCGM/CGMW, 269 pp.

Fischer J, Voigt S, Franz M, Schneider JW, Joachimski MM, Tichomirowa M, Götze J and Furrer H (2012) Palaeoenvironments of the late Triassic Rhaetian Sea: implications from oxygen and strontium isotopes of hybodont shark teeth. Palaeogeography, Palaeoclimatology, Palaeoecology 353–355, 60–72.

Folk RL (1974) The Petrology of Sedimentary Rocks. Austin, Texas: Hemphill's, 183 pp.

François T, Barbarand J and Wyns R (2020) Lower Cretaceous inversion of the European Variscan basement: record from the Vendée and Limousin (France). International Journal of Earth Sciences 109, 1837–52. doi: 10.1007/s00531-020-01875-z.

Goldsmith PJ, Hudson G and van Veen P (2003) Triassic. In The Millennium Atlas: Petroleum Geology of the Central and Northern North Sea (eds D Evans, C Graham, A Armour and P Bathurst), pp. 105–27. Geological Society of London, 389 pp.

Herreros MI and Ormö J (2022) Marine impacts: sedimentological fingerprint of event magnitude. Geology 50(12), 1331–1335. doi: 10.1130/G50250.1.

Horne A (2016) (U–Th)/He, U/Pb, and radiation damage dating of the Rochechouart-Chassenon impact structure. Master thesis, Arizona State University, USA, 63 pp. Published thesis.

Jourdan F, Reimold WU and Deutsch A (2012) Dating terrestrial impact structures. Elements 8, 49–53.

Jourdan F, Renne PR and Reimold WU (2007) The problem of inherited $^{40}Ar^{*}$ in dating impact glass by $^{40}Ar/^{39}Ar$ geochronology: evidence from the Tswaing crater (South Africa). Geochimica et Cosmochimica Acta 71, 1214–31.

Kelley SP and Spray JG (1997) A Late Triassic age for the Rochechouart impact structure, France. Meteoritics and Planetary Science 32, 629–36.

King DT Jr, Ormö J, Petruny LW and Neathery TL (2006) Role of water in the formation of the Late Cretaceous Wetumpka impact structure, inner Gulf Coastal Plain of Alabama, USA. Meteoritics and Planetary Science 41, 1625–31. doi: 10.1111/j.1945-5100.2006.tb00440.x.

Kraut F and French BM (1971) The Rochechouart meteorite impact structure, France; preliminary geological results. Journal of Geophysical Research 76, 5407–13.

Lambert P (1977) The Rochechouart crater: shock zoning study. Earth and Planetary Science Letters 35, 258–68.

Lambert P et al. (58 authors) (2018) Rochechouart 2017-drilling campaign: first results. Lunar and Planetary Science 49, #1954 (Abstract).

Lambert P and the CIRIR Consortium (60 authors) (2019) The Rochechouart 2017-Cores Rescaled: Major Features. 50th Lunar and Planetary Science Conference, held 18-22 March, 2019 at The Woodlands, Texas. LPI Contribution No. 2132, #2005.

Lambert P (2010) Target and impact deposits at Rochechouart impact structure, France. In Large Meteorite Impacts and Planetary Evolution IV (eds RL Gibson and WU Reimold), pp. 509–41. Geological Society of America Special Papers 465.

Le Pochat G, Floc'h JP, Platel JP and Recoing M (1986) Notice explicative, Carte géol. France (1/50 000) feuille Montbron (710). Orléans: BRGM, 47 pp.

Mader D (1992) Evolution of Palaeoecology and Palaeoenvironment of Permian and Triassic Fluvial Basins in Europe. Stuttgart/New York: Gustav Fischer Verlag, 738 pp.

Merzeraud G, Hoffert M, Verdier F and Rauscher R (1999) Architecture and preservation of silico-clastic reservoirs in lower Liassic deposits of the southwestern part of the Paris Basin: example of Chemery field in the Sologne region (bore-hole data of Gaz de France). Bulletin de la Société Géologique de France 170, 741–57.

Merzeraud G, Rauscher R, Hoffert M and Verdier F (2000) Stacking pattern and stratigraphic distortion of genetic sequences in a restricted marine environment. Bulletin de la Société Géologique de France 171, 341–53.

Ormö J, Gulick SPS, Whalen MT, King DT Jr, Sturkell E and Morgan J (2021) Assessing event magnitude and target water depth for marine-target impacts: ocean resurge deposits in the Chicxulub M0077A drill core compared. Earth and Planetary Science Letters 564. doi: 10.1016/j.epsl. 2021.116915.

Ormö J, Lepinette A, Sturkell E, Lindström M, Housen KR and Holsapple KA (2010) The water resurge at marine-target impact craters analyzed with a combination of low-velocity impact experiments and numerical simulations. In Large Meteorite Impacts and Planetary Evolution IV (eds RL Gibson and WU Reimold), pp. 81–101. Geological Society of America Special Papers 465.

Ormö J, Sturkell E, Horton JW Jr, Powars DS and Edwards LE (2009) Comparison of clast frequency and size in the resurge deposits at the Chesapeake Bay impact structure (Eyreville-A and Langley cores): clues to the resurge process. In The ICDP–USGS Deep Drilling Project in the Chesapeake Bay Impact Structure: Results from the Eyreville Core Holes (eds GS Gohn, C Koeberl, KG Miller and WU Reimold), pp. 617–32. Boulder, CO, USA: Geological Society of America Special Papers 458.

Ormö J, Sturkell E and Lindström M (2007) Sedimentological analysis of resurge deposits at the Lockne and Tvären craters: clues to flow dynamics. Meteoritics and Planetary Science 42, 1929–44.

Osinski GR and Ferrière L (2016) Shatter cones: (mis)understood? Science Advances 2, e1600616. doi: 10.1126/sciadv.1600616.

Osinski GR, Grieve RAF, Hill PJA, Simpson SL, Cockell C, Christeson GL, Ebert M, Gulick SPS, Melosh HJ, Riller U, Tikoo SM and Wittmann A (2020) Explosive interaction of impact melt and seawater following the Chicxulub impact event. Geology 48, 108–12. doi: 10.1130/G46783.1.

Pohl J, Ernstson K and Lambert P (1978) Gravity measurements in the Rochechouart impact structure (France). Meteoritics 13, 601–4.

Rasmussen C, Stockli DF, Erickson TM and Schmieder M (2020) Spatial U-Pb age distribution in shock-recrystallized zircon: a case study from the Rochechouart impact structure, France. Geochimica et Cosmochimica Acta 273, 313–30. doi: 10.1016/j.gca.2020.01.017.

Rauscher R, Merzeraud G and Schuler M (1992) Biostratigraphie, environnements et cortèges de dépôts dans le Lias inférieur de Sologne (S.W. du Bassinde Paris). Review of Palaeobotany and Palynology 71, 17–35. doi: 10.1016/0034-6667(92)90156-B.

Reimold WU and Oskierski W (1987) The Rb-Sr-age of the Rochechouart impact structure, France, and geochemical constraints on impact melt-target rock-meteorite compositions. In Research in Terrestrial Impact Structures (ed J Pohl), pp. 94–114. Wiesbaden: Vieweg Þ Teubner Verlag.

Renne PR, Balco G, Ludwig KR, Mundil R, Min K (2011) Response to the comment by W.H. Schwarz et al. on "Joint determination of 40K decay constants and 40Ar*/40K for the Fish Canyon sanidine standard, and improved accuracy for 40Ar/39Ar geochronology" by Paul R. Renne et al. (2010). Geochimica et Cosmochimica Acta 75, 5097–100.

Schmieder M, Buchner E, Schwarz WH, Trieloff M and Lambert P (2010) A Rhaetian $^{40}Ar/^{39}Ar$ age for the Rochechouart impact structure (France) and implications for the latest Triassic sedimentary record. Meteoritics and Planetary Science 45, 1225–42.

Schmieder M, Jourdan F, Tohver E and Cloutis EA (2014) $^{40}Ar/^{39}Ar$ age of the Lake Saint Martin impact structure (Canada): unchaining the Late Triassic terrestrial impact craters. Earth and Planetary Science Letters 406, 37–48.

Scotese CR and Schettino A (2017) Late Permian-Early Jurassic paleogeography of Western Tethys and the world. In Permo-Triassic Salt Provinces of Europe, North Africa and the Atlantic Margins: Tectonics and Hydrocarbon Potential (eds JI Soto, JF Flinch and G Tari), pp. 57–95. Amsterdam: Elsevier

Simms MJ (2007) Uniquely extensive soft-sediment deformation in the Rhaetian of the UK: evidence for earthquake or impact? Palaeogeography, Palaeoclimatology, Palaeoecology 244, 407–23.

Sturkell E, Ormö J and Lepinette A (2013) Early modification stage (pre-resurge) sediment mobilization in the Lockne concentric, marine-target crater, Sweden. Meteoritics and Planetary Science 48, 321–38. doi: 10.1111/ maps.12058.

Tagle R, Schmitt RT and Erzinger J (2009) Identification of the projectile component in the impact structures Rochechouart, France and Sääksjärvi, Finland: implications for the impactor population for the Earth. Geochimica et Cosmochimica Acta 73, 4891–906.

Therriault AM and Lindström M (1995) Planar deformation features in quartz grains from the resurge deposit of the Lockne structure, Sweden. Meteoritics and Planetary Science 30, 700–3.

Vallance JW (2000) Lahars. In Encyclopedia of Volcanoes (ed H Sigurdsson), pp. 601–16. San Diego, California: Academic Press.

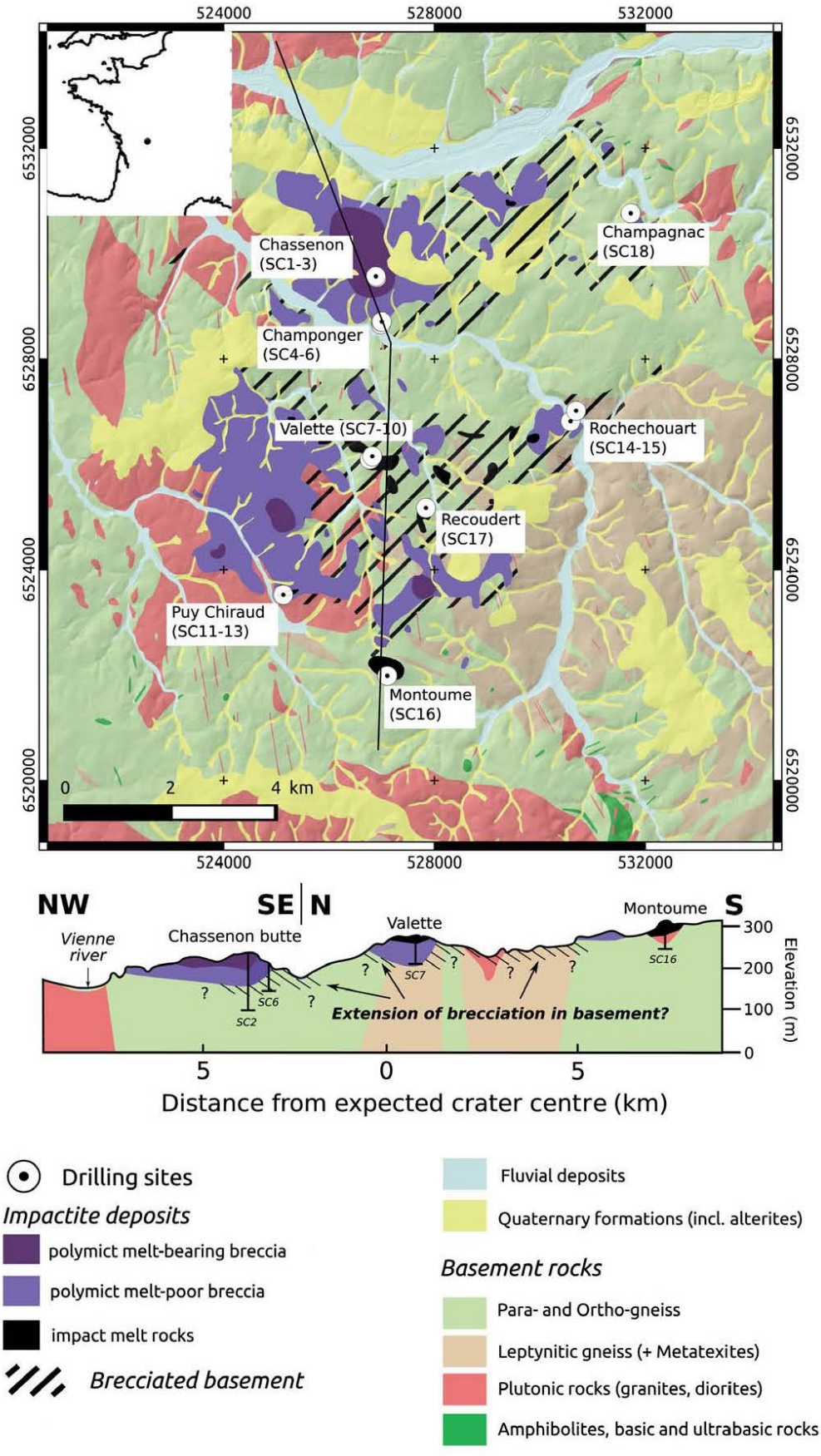

Fig. 1. Geological map of the Rochechouart impact structure with locations of core hales from the 2017 drilling campaign (Lambert et al. 2018).

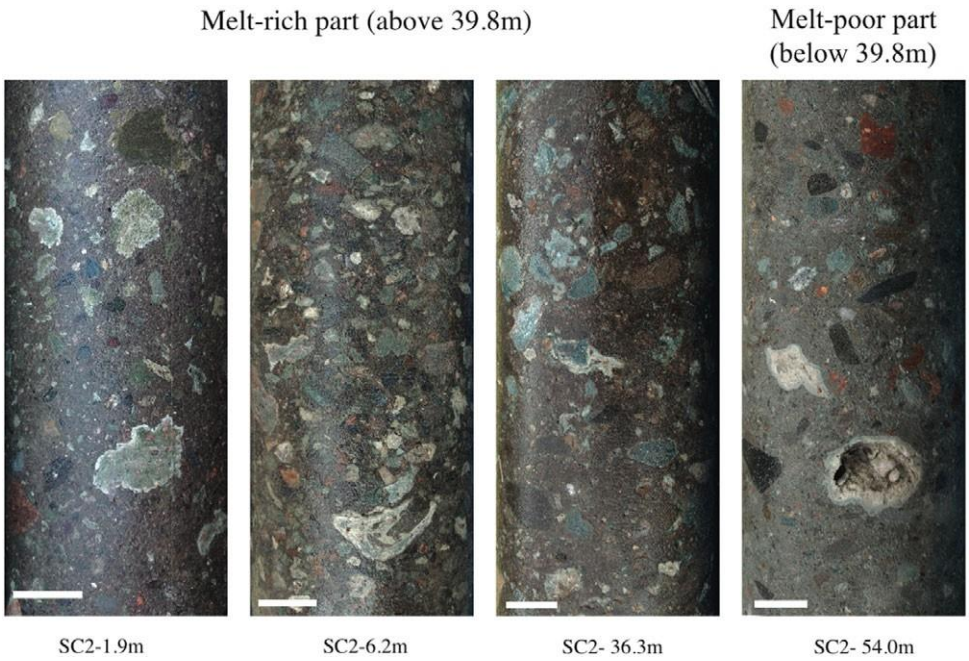

Fig. 2. Representative core photos of the suevite (melt clast breccia) of the SC2 core. Lambert (2010) divides the suevite into an upper, melt-rich part and a lower melt-poor part. Scale bars are 2 cm.

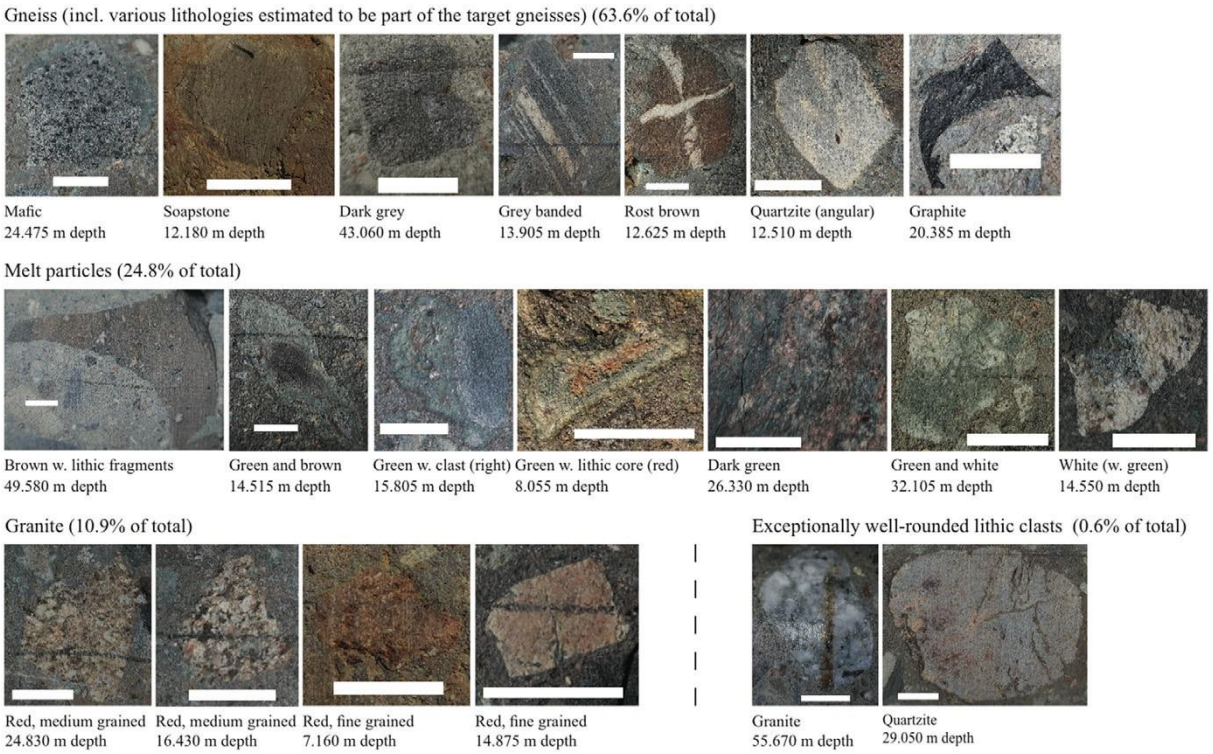

Fig. 3. Clast classification. Scale bars are 1 cm.

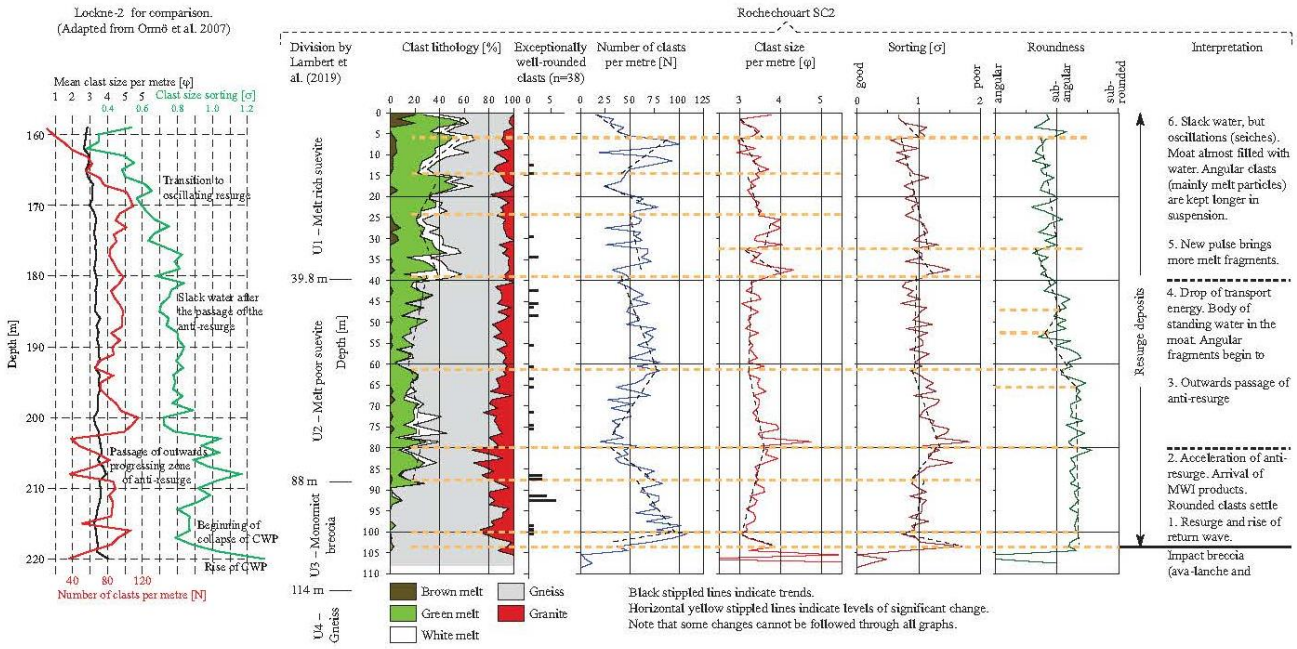

Fig. 4. Graphs showing variations in granulometry and clast lithology in the graded suevite of the SC2 core. Inset to the left are graphs from a similar logging by Ormö et al. (2007) of the Lockne-2 core at the marine target Lockne crater, Sweden. The interpretation to the right is based on comparisons with line-logging results from similar deposits at several other impact craters (e.g. Ormö et al. 2007, 2009, 2021; Sturkell et al. 2013; De Marchi et al. 2019), but Lockne-2 is considered to provide the best analogy to the Rochechouart SC2 core.

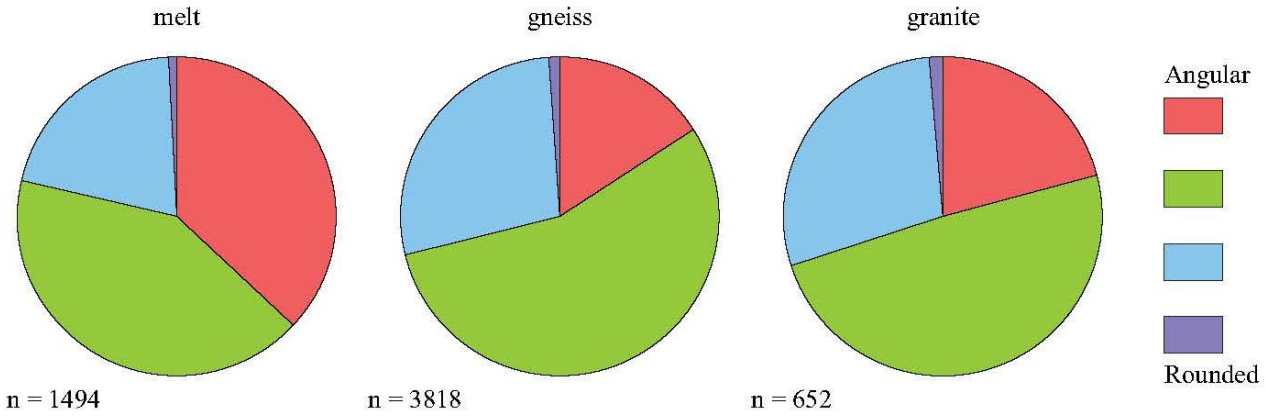

Fig. 5. Degree of roundness of the main clast lithologies except EWRLC. Melt particles are notably the most angular.

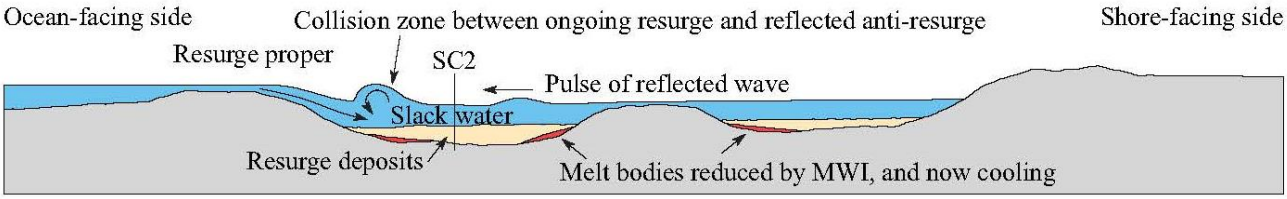

Fig. 6. Schematic process reconstruction of Stage 5 of the resurge at the Rochechouart crater (Fig. 4). As currently the size and morphology of the fresh crater are not known, the cross-section is only meant to be seen as conceptual in order to explain the various interpreted mechanisms of the resurge process, e.g. collision of flow, MWI, pulse of reflected wave. The conceptual cross-section chosen here is that of a complex crater, as the consensus of current published estimates is that of a crater with a diameter much wider than the transition from simple to complex morphology. However, in a much larger option, the central uplift indicated here could be replaced by a peak ring. The location of the drill hole SC2 is indicated, as well as the likely nearshore position of the crater.

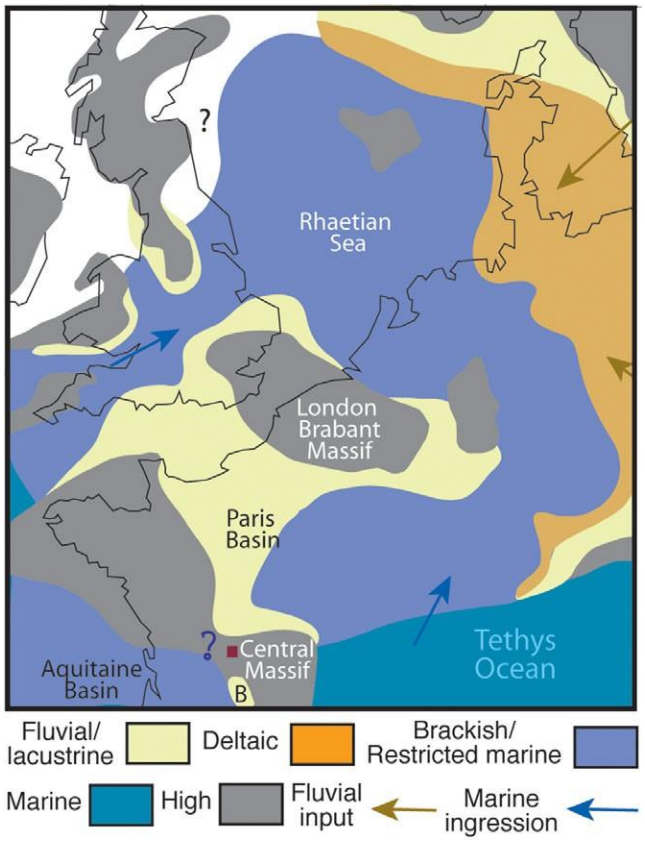

Fig. 7. Rhaetian palaeogeographic reconstruction of Fischer et al. (2012) modified from Bourquin et al. (1997, 2002). B: Brive area.

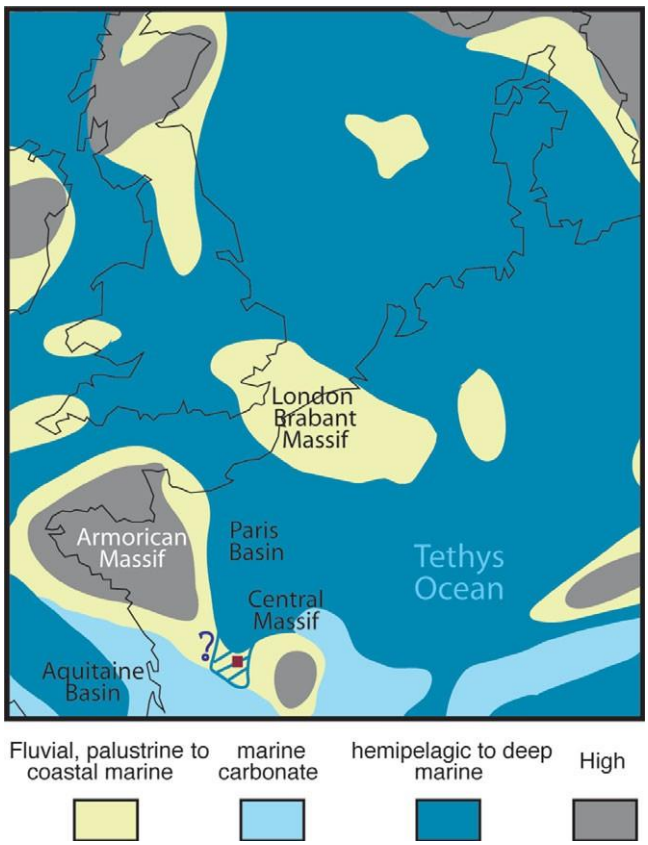

Fig. 8. Early Jurassic palaeogeographic reconstruction (Hettangian and Sinemurian). Modified from Dercourt et al. (2000) and Scotese and Schettino (2017).